
Efficiently Predicting Protein Stability Changes Upon Single-point Mutation with Large Language Models

Yijie Zhang^{1,3*}, Zhangyang Gao^{1,2*}, Cheng Tan^{1,2*}, and Stan Z. Li^{1†}
¹AI Lab, Research Center for Industries of the Future, Westlake University
²Zhejiang University
³McGill University
yj.zhang@mail.mcgill.ca
{tancheng,gaozhangyang,stan.zq.li}@westlake.edu.cn

Abstract

Predicting protein stability changes induced by single-point mutations has been a persistent challenge over the years, attracting immense interest from numerous researchers. The ability to precisely predict protein thermostability is pivotal for various subfields and applications in biochemistry, including drug development, protein evolution analysis, and enzyme synthesis. Despite the proposition of multiple methodologies aimed at addressing this issue, few approaches have successfully achieved optimal performance coupled with high computational efficiency. Two principal hurdles contribute to the existing challenges in this domain. The first is the complexity of extracting and aggregating sufficiently representative features from proteins. The second refers to the limited availability of experimental data for protein mutation analysis, further complicating the comprehensive evaluation of model performance on unseen data samples. With the advent of Large Language Models (LLM), such as the ESM models in protein research, profound interpretation of protein features is now accessibly aided by enormous training data. Therefore, LLMs are indeed to facilitate a wide range of protein research. In our study, we introduce an ESM-assisted efficient approach that integrates protein sequence and structural features to predict the thermostability changes in protein upon single-point mutations. Furthermore, we have curated a dataset meticulously designed to preclude data leakage, corresponding to two extensively employed test datasets, to facilitate a more equitable model comparison.

1 Introduction

Proteins are crucial biomolecules in organisms [1], essential for catalyzing metabolic reactions [2, 3], DNA replication [4], responding to stimuli [5], providing cellular structure [6], and transporting molecules [7]. Over the past decades, advancements in electron microscopy have allowed researchers to study protein structure and functions at the molecular level, leading to the emergence of Protein Engineering [8, 9]. This field, as well as other approaches towards different biomolecules, focuses on discovering [10, 11, 12, 13], designing [14, 15, 16, 17, 18, 19, 20, 21, 22, 23], and realizing molecules with specific functions or properties [24, 25, 26, 27, 28, 29, 30, 31, 32], contributing significantly to biochemistry and medicine. Since any change in the components of protein molecules could be considered a chemical reaction, the thermostability could be interpreted as the tendency that which a mutation is about to happen, usually denoted as the subtraction of Gibbs folding free energy ΔG for

*Equal contribution.

†Corresponding author.

a pair of wild and mutated proteins 1 [33]. A higher $\Delta\Delta G$ value indicates a more stable protein [34].

$$\Delta\Delta G_{MW} = \Delta G_M - \Delta G_W \tag{1}$$

where M denotes mutated type and W denotes wild type.

Previous researchers have proposed several approaches to predict the $\Delta\Delta G$ by exploring molecular dynamics to simulate protein folding patterns [35, 36], analyzing statistical relationships on the mutation pairs [37, 38, 39, 40], and utilizing molecular modeling techniques [41, 42]. The emergence of machine learning has brought this field ample possibilities [43, 44]. In general, machine learning-based protein thermostability prediction could be diversified into two categories. (i) Sequence-based methods mainly aim to extract useful features from protein sequences [45, 46, 47, 48, 49, 50, 51, 52]. (ii) Structure-based methods aim to extract the structural variances to predict the $\Delta\Delta G$ [53, 54, 55, 56, 57, 58, 59, 60, 61, 62, 63, 64, 65]. Notably, PROSTATA [49] fine-tuned pretrained protein large language model to predict protein mutational effects and achieved considerable results.

In reviewing prior methodologies in this domain, two significant challenges emerge. First, achieving a standardized comparison among models remains problematic, even with the recent introduction of major testing datasets. This issue is exacerbated by many methods relying on private training datasets, some of which are not publicly accessible, hindering comprehensive comparisons. Moreover, as delineated in Appendix A, certain public datasets exhibit information leakage when compared with common testing datasets. The second challenge lies in maintaining an equilibrium between model accuracy, computational demands, and reproducibility. For instance, while structure-based methods may outperform their sequence-based counterparts, they often come with substantial computational costs, especially when utilizing advanced protein structure predictors like AlphaFold2 [66] and Rosetta [67] to generate tertiary structures.

In this work, we present two primary contributions to address these challenges. Firstly, we constructed a cleaned protein single-point dataset containing protein wild and mutated sequences aligned with the backbone atom coordinates extracted from the PDB file, and the corresponding $\Delta\Delta G$ values. The dataset has two subsets, each filtering out similar structures corresponding to the S669 and Ssym datasets. Hence, researchers can now integrate experimental sequential and structural features, while also ensuring fair comparisons using the filtered training and test datasets, thereby eliminating information leakage. Secondly, we proposed an ESM-augmented model to predict the $\Delta\Delta G$ upon protein single-point mutation accurately and effectively. The source code and the datasets will be available publicly soon.

2 Method

2.1 Dataset

In this paper, we introduce a novel training dataset characterized by two principal contributions. First, we meticulously align sequences and structures, the latter representing the coordinates of the backbone atom within each amino acid. This alignment results in clean and precise sequence-structure pairs, ready for further applications. Second, we ensure no information leakage between our dataset and the widely recognized test datasets, specifically, the S669 [68] and Ssym datasets [69]. Any structures bearing resemblance to those within the mentioned datasets have been diligently omitted to maintain integrity and uniqueness in our collection. Notably, we proposed two subsets corresponding to each test dataset to ensure not lose too many samples for training.

We derived our initial dataset from PROSTATA [49], an aggregation of various datasets that have been utilized in preceding methodologies. This aggregation allowed for the selection of samples under unified experimental conditions. The dataset we propose encompasses both wild and mutated sequences, along with corresponding $\Delta\Delta G$ values, comprising 10544 samples, including reverse mutations. To preclude any potential information leakage between the training and test datasets, we employed the TM-Score, a measure signifying structural similarity amongst proteins, and analyzed it between each sample in both datasets. We adhered to the threshold and set it as an average score of 0.5 [70]. Consequently, samples exhibiting a score exceeding this threshold, in comparison to any structures within the testing dataset, were excluded from our dataset. We have provided a comparative analysis in the Appendix A to facilitate our structure selection.

Upon acquiring the refined training dataset, we extracted the backbone coordinates from the corresponding PDB files and aligned them with the sequences. This alignment aimed to generate coherent

structure-sequence pairs, streamlining the feature extraction process. For the purposes of our experiment, we adopted the coordinates of the C_α atom to represent the structure of each residue. However, discrepancies in alignment were observed during this process. To address these misalignments, we devised a checking algorithm to discern and select coherent and applicable sequence-structure pairs for subsequent experimentation. The specifics of this algorithm are delineated in the Appendix A.1. Finally, we maintained two subsets for training purposes, with regards to evaluating the model performance on S669 or Ssym datasets.

2.2 Model Details

We separate the process of predicting $\Delta\Delta G$ for single-point mutations into two steps. As per Equation 1, we can predict the ΔG value for each protein and then find the difference between these predictions to get $\Delta\Delta G$. Building on the approach from CDConv [71], we have integrated both sequence and structural information to improve our predictions. Given the lack of mutated structures, we have used the structures of wild proteins as our structural inputs, an approach supported by SCONES [65], showing minimal structural changes in unstable protein mutations.

In particular, we used CDConv [71] for predicting the ΔG value due to its innovative approach and well-structured graph convolutional network. Also, we have added the sequential embedding from the ESM-2 650M UR50D model to our input, enhancing our feature extraction capabilities. More details on the proposed strategies are provided below:

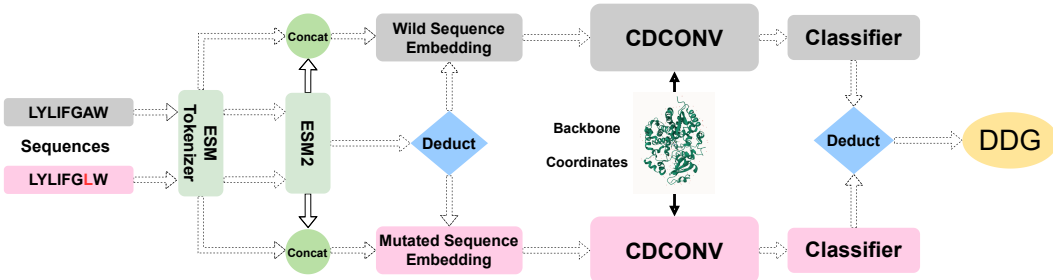


Figure 1: The architecture of our proposed model

System architecture Our model receives sequence-structure pairs for both wild-type and mutated-type as input. The ESM-assisted Continuous Graph Convolutional Network is independently employed on each input to assimilate sequential and structural features into a coherent embedding. Subsequently, we deduct one embedding from the other, transforming it into a one-dimensional prediction via a nonlinear classifier. The detailed system pipeline is shown in Figure 1.

ESM augmented variance enhancement To streamline the extraction of sequence features, we employed and froze the ESM-2 model to derive a sequential representation matrix for each mutation pair. Subsequently, the obtained embedding was concatenated with the sequence embedding, serving as the input for the graph neural networks. Given the scarce feature variances induced by single-point protein mutations, we also incorporated the difference between the mutated and wild sequence embeddings into both inputs to enhance the feature variance. We have presented the sample input generation process for either mutated or wild type in Algorithm 1. Consequently, this integration aids in accentuating the subtle alterations caused by mutations, allowing the model to effectively discern and learn from the nuanced differences between the mutated and wild-type sequences.

Algorithm 1 Model Input Generation

$$\begin{aligned}
 SeqInput &\leftarrow \text{Concat}(SeqEmbed_{ESM}, SeqEmbed_{CDConv}) \\
 DiffEmbed &\leftarrow SeqInput_{mut} - SeqInput_{wild} \\
 FinalSeqInput &\leftarrow \text{Concat}(SeqInput, DiffEmbed)
 \end{aligned}$$

Loss function In Appendix A.3, the distribution of $\Delta\Delta G$ values reveals that the vast majority of samples are at a range between $[-5, 5]$. Therefore, in order to better conceive the effect of major cases, we adopted the concept of Huber Loss, as denoted in Equation 2

$$L_\delta(y, f(x)) = \begin{cases} \frac{1}{2}(y - f(x))^2 & \text{for } |y - f(x)| \leq \delta \\ \delta|y - f(x)| - \frac{1}{2}\delta^2 & \text{otherwise} \end{cases} \quad (2)$$

Where L_δ represents the Huber Loss, y is the true value, $f(x)$ is the predicted value, and δ is a threshold set to 1.0.

3 Experiment Details

Datasets We assess the effectiveness of our method utilizing two distinct test datasets: the S669 dataset [68] and the Ssym dataset [69]. The details of curating the training dataset are illustrated in Appendix A.1.

- **S669 Dataset** is a novel test dataset that is less similar to conventional training sets, including 669 mutations. In order to better analyze the pattern of protein point mutation, we compiled S669_r dataset, which is a reverse in $\Delta\Delta G$ value and the mutation points, based on the assumption that such reaction is reversible [72]. For better evaluation, we employed a refined training dataset, encompassing 6951 samples. These samples exhibit no structural similarity to those within the S669 dataset, ensuring the robustness and reliability of our assessment.
- **Ssym Dataset** consists of an equal distribution of stabilizing and destabilizing mutations, each having 342 samples. Consequently, we have partitioned the dataset into Ssym and Ssym_r subsets, including allocated stabilizing and destabilizing mutations following previous approaches [49, 69], respectively. To evaluate our model performance on these datasets, we utilize an analogous cleaned training dataset containing 6080 samples. These training samples are subjected to have no information leakage to the Ssym datasets, maintaining consistency in the evaluation process.

Metrics We chose to employ the Pearson Coefficient (PCC), Root Mean Square Error (RMSE), and Mean Absolute Error (MAE) as metrics to provide a comprehensive assessment of our model’s performance. The Pearson Coefficient offers insights into the linear correlation between predicted and true values, RMSE accentuates larger errors providing a focus on substantial inaccuracies, and MAE presents a clear picture of the model’s predictive capability by measuring the average magnitude of the errors.

Baseline Models We mainly utilized PROSTATA [49] for comparison. We trained the model following the source code on two conditions. (i) We trained with the original sequence dataset that only excludes similar samples from each of the test datasets. For the S669, our filtered training dataset contains 7137 samples, for the Ssym, it contains 6278. (ii) We trained with our proposed dataset, which extracts the filtered sequential information from the structure-sequence pairs. For the S669, the training dataset has 6951 samples while for the Ssym, it has 6080. We reported the results and compared them with our model in Section 3.1. Besides, we compared our model’s performance with previous works in Appendix C.

3.1 Evaluation on S669 and Ssym datasets

Using our proposed dataset, we trained the model using two training datasets separately. One is for evaluating the model performance on the S669 and S669_r datasets, and the other is for the Ssym and Ssym_r datasets. In order to promote a fair utilization of all the data samples, we used a 5-fold cross-validation process for model training. The experiments were conducted under multiple hyperparameter combinations. In this way, we found the best hyperparameters for our model, illustrated in Appendix B. Then, we evaluated the performance of the model on the testing dataset by testing the model performance in each fold and averaging the 5 results. The results from both the original and reversed datasets are jointly presented in Tables 1 and 2, providing a more comprehensive assessment. Together with the results of model performance under two testing datasets, we evaluated the average per-epoch training time of PROSTATA and our model under the same conditions.

Table 1: The evaluation results on the S669 and S669_r datasets.

Method(Samples)	S669			S669_r			Runtime(minutes)
	PCC \uparrow	RMSE \downarrow	MAE \downarrow	PCC \uparrow	RMSE \downarrow	MAE \downarrow	
PROSTATA(7137)	0.48	1.46	1.02	0.47	1.45	1.00	-
PROSTATA(6951)	0.47	1.51	1.02	0.46	1.47	1.00	28.2(14.85 \times)
Ours(6951)	0.51	1.46	1.07	0.51	1.46	1.07	1.9(1.00 \times)

Table 2: The evaluation results on the Ssym and Ssym_r datasets.

Method(Samples)	Ssym			Ssym_r			Runtime(minutes)
	PCC \uparrow	RMSE \downarrow	MAE \downarrow	PCC \uparrow	RMSE \downarrow	MAE \downarrow	
PROSTATA(6278)	0.47	1.42	1.01	0.48	1.42	1.01	-
PROSTATA(6080)	0.50	1.45	1.02	0.46	1.51	1.07	23.9(14.94 \times)
Ours(6080)	0.47	1.45	1.05	0.47	1.45	1.05	1.6(1.00 \times)

From the results revealed, it could be concluded that for both testing datasets, the PROSTATA method with reduced samples shows a slight increase in RMSE and MAE compared to its counterpart, indicating a minor compromise in prediction accuracy. Notably, our proposed method consistently performs on par with the PROSTATA method with similar sample sizes, while drastically improving the runtime efficiency, since our method freezes the gradient of the ESM model thus it does not need to update the parameters in it. In both testing datasets, our method achieves nearly 15 times faster processing than PROSTATA without compromising much on the accuracy metrics. These results highlight the efficacy of our method in balancing accuracy and computational efficiency.

3.2 Ablation Study

To elucidate the contribution of each component of our model, we performed a detailed ablation study. From Table 3, our proposed model demonstrates the best performance across both datasets in all the metrics. When we remove the ESM embedding, there is a drastic decline in performance, especially in PCC values, which drop to 0.25 and 0.31 for S669 and Ssym, respectively. This suggests that ESM embedding plays a pivotal role in capturing the intricate patterns in the data. On the other hand, excluding the CDConv embedding results in a more subtle performance degradation. Although the decline is not as pronounced as in the ESM ablation, it is still noteworthy, particularly in the PCC metric. This indicates that while CDConv embedding contributes to the model’s performance, the ESM embedding appears to be more critical for the model’s efficacy.

Table 3: The ablation study of our model on two datasets.

Method	Metrics					
	PCC \uparrow		RMSE \downarrow		MAE \downarrow	
	S669	Ssym	S669	Ssym	S669	Ssym
Ours	0.51	0.47	1.46	1.45	1.07	1.05
w/o ESM embedding	0.25	0.31	1.90	1.80	1.44	1.32
w/o CDConv embedding	0.48	0.39	1.54	1.54	1.13	1.12

4 Conclusion and Discussion

In our paper, we conducted thorough research on predicting the $\Delta\Delta G$ of protein single-point mutation. We assembled a dataset of aligned sequence-structure pairs, ensuring no information leakage with prevalent testing datasets to maintain fairness in model comparison and evaluation. Additionally, we introduced an ESM-augmented prediction model, leveraging both sequence and structure features, demonstrating exemplary performance across all testing datasets.

In our approach, the ESM model is frozen during the acquisition of input embeddings, which are subsequently stored locally, enhancing the model’s computational efficiency. This approach relies

solely on authentic PDB files, avoiding the use of computational protein structure predictors like AlphaFold2, making it more accessible for researchers to conduct experiments independently.

However, our approach has its limitations. The refinement of sequence selection algorithms is crucial during the cleaning of sequences with structural features, and further investigations into biochemical aspects are necessary to improve the robustness and interoperability of the model.

References

- [1] Martin Karplus and John Kuriyan. Molecular dynamics and protein function. *Proceedings of the National Academy of Sciences*, 102(19):6679–6685, 2005.
- [2] Alessandro Michelucci, Thekla Cordes, Jenny Ghelfi, Arnaud Pailot, Norbert Reiling, Oliver Goldmann, Tina Binz, André Wegner, Aravind Tallam, Antonio Rausell, et al. Immune-responsive gene 1 protein links metabolism to immunity by catalyzing itaconic acid production. *Proceedings of the National Academy of Sciences*, 110(19):7820–7825, 2013.
- [3] D Michael Gill and Roberta Meren. Adp-ribosylation of membrane proteins catalyzed by cholera toxin: basis of the activation of adenylate cyclase. *Proceedings of the National Academy of Sciences*, 75(7):3050–3054, 1978.
- [4] Stephen J Benkovic, Ann M Valentine, and Frank Salinas. Replisome-mediated dna replication. *Annual review of biochemistry*, 70(1):181–208, 2001.
- [5] Nelo Eidy Zanchi and Antonio Herbert Lancha. Mechanical stimuli of skeletal muscle: implications on mtor/p70s6k and protein synthesis. *European journal of applied physiology*, 102:253–263, 2008.
- [6] E Hesper Rego, Lin Shao, John J Macklin, Lukman Winoto, Göran A Johansson, Nicholas Kamps-Hughes, Michael W Davidson, and Mats GL Gustafsson. Nonlinear structured-illumination microscopy with a photoswitchable protein reveals cellular structures at 50-nm resolution. *Proceedings of the National Academy of Sciences*, 109(3):E135–E143, 2012.
- [7] Thomas Zeuthen. Water-transporting proteins. *Journal of Membrane Biology*, 234:57–73, 2010.
- [8] Bozhen Hu, Jun Xia, Jiangbin Zheng, Cheng Tan, Yufei Huang, Yongjie Xu, and Stan Z. Li. Protein language models and structure prediction: Connection and progression, 2022.
- [9] Paul J Carter. Introduction to current and future protein therapeutics: a protein engineering perspective. *Experimental cell research*, 317(9):1261–1269, 2011.
- [10] Zhangyang Gao, Cheng Tan, and Stan Z Li. Vqpl: Vector quantized protein language. *arXiv preprint arXiv:2310.04985*, 2023.
- [11] Kevin M Ulmer. Protein engineering. *Science*, 219(4585):666–671, 1983.
- [12] Tom W Muir, Dolan Sondhi, and Philip A Cole. Expressed protein ligation: a general method for protein engineering. *Proceedings of the National Academy of Sciences*, 95(12):6705–6710, 1998.
- [13] Stefan Lutz and Uwe Theo Bornscheuer. *Protein engineering handbook*. John Wiley & Sons, 2012.
- [14] Zhangyang Gao, Cheng Tan, and Stan Z Li. Pifold: Toward effective and efficient protein inverse folding. *arXiv preprint arXiv:2209.12643*, 2022.
- [15] Cheng Tan, Zhangyang Gao, Jun Xia, Bozhen Hu, and Stan Z Li. Global-context aware generative protein design. In *ICASSP 2023-2023 IEEE International Conference on Acoustics, Speech and Signal Processing (ICASSP)*, pages 1–5. IEEE, 2023.
- [16] John Ingraham, Vikas Garg, Regina Barzilay, and Tommi Jaakkola. Generative models for graph-based protein design. In H. Wallach, H. Larochelle, A. Beygelzimer, F. d’Alché-Buc, E. Fox, and R. Garnett, editors, *Advances in Neural Information Processing Systems*, volume 32, pages 15820–15831. Curran Associates, Inc., 2019.
- [17] Bowen Jing, Stephan Eismann, Patricia Suriana, Raphael John Lamarre Townshend, and Ron Dror. Learning from protein structure with geometric vector perceptrons. In *International Conference on Learning Representations*, 2021.
- [18] Zhangyang Gao, Cheng Tan, Stan Li, et al. Alphadesign: A graph protein design method and benchmark on alphafolddb. *arXiv preprint arXiv:2202.01079*, 2022.

- [19] Cheng Tan, Zhangyang Gao, and Stan Z Li. Rfold: Towards simple yet effective rna secondary structure prediction. *arXiv preprint arXiv:2212.14041*, 2022.
- [20] Alexey Strokach, David Becerra, Carles Corbi-Verge, Albert Perez-Riba, and Philip M. Kim. Fast and flexible protein design using deep graph neural networks. *Cell Systems*, 11(4):402–411.e4, 2020.
- [21] Yue Cao, Payel Das, Vijil Chenthamarakshan, Pin-Yu Chen, Igor Melnyk, and Yang Shen. Fold2seq: A joint sequence(1d)-fold(3d) embedding-based generative model for protein design. In Marina Meila and Tong Zhang, editors, *Proceedings of the 38th International Conference on Machine Learning*, volume 139 of *Proceedings of Machine Learning Research*, pages 1261–1271. PMLR, 18–24 Jul 2021.
- [22] Cheng Tan, Yijie Zhang, Zhangyang Gao, Hanqun Cao, and Stan Z. Li. Hierarchical data-efficient representation learning for tertiary structure-based rna design, 2023.
- [23] Zhangyang Gao, Cheng Tan, and Stan Z Li. Knowledge-design: Pushing the limit of protein design via knowledge refinement. *arXiv preprint arXiv:2305.15151*, 2023.
- [24] Wengong Jin, Regina Barzilay, and Tommi Jaakkola. Junction tree variational autoencoder for molecular graph generation. In *International conference on machine learning*, pages 2323–2332. PMLR, 2018.
- [25] Cheng Tan, Zhangyang Gao, and Stan Z Li. Target-aware molecular graph generation. In *Joint European Conference on Machine Learning and Knowledge Discovery in Databases*, pages 410–427. Springer, 2023.
- [26] Zhangyang Gao, Cheng Tan, Jun Xia, and Stan Z Li. Co-supervised pre-training of pocket and ligand. In *Joint European Conference on Machine Learning and Knowledge Discovery in Databases*, pages 405–421. Springer, 2023.
- [27] Yangtian Zhang, Huiyu Cai, Chence Shi, Bozita Zhong, and Jian Tang. E3bind: An end-to-end equivariant network for protein-ligand docking. *arXiv preprint arXiv:2210.06069*, 2022.
- [28] Cheng Tan, Zhangyang Gao, and Stan Z Li. Cross-gate mlp with protein complex invariant embedding is a one-shot antibody designer. *arXiv e-prints*, pages arXiv–2305, 2023.
- [29] Mikołaj Sacha, Mikołaj Błaz, Piotr Byrski, Paweł Dabrowski-Tumanski, Mikołaj Chrominski, Rafał Loska, Paweł Włodarczyk-Pruszynski, and Stanisław Jastrzebski. Molecule edit graph attention network: modeling chemical reactions as sequences of graph edits. *Journal of Chemical Information and Modeling*, 61(7):3273–3284, 2021.
- [30] Vignesh Ram Somnath, Charlotte Bunne, Connor Coley, Andreas Krause, and Regina Barzilay. Learning graph models for retrosynthesis prediction. *Advances in Neural Information Processing Systems*, 34:9405–9415, 2021.
- [31] Zhangyang Gao, Cheng Tan, Lirong Wu, and Stan Z Li. Semiretro: Semi-template framework boosts deep retrosynthesis prediction. *arXiv preprint arXiv:2202.08205*, 2022.
- [32] Zhangyang Gao, Xingran Chen, Cheng Tan, and Stan Z Li. Motifretro: Exploring the combinability-consistency trade-offs in retrosynthesis via dynamic motif editing. *arXiv preprint arXiv:2305.15153*, 2023.
- [33] Nobuhiko Tokuriki and Dan S Tawfik. Stability effects of mutations and protein evolvability. *Current opinion in structural biology*, 19(5):596–604, 2009.
- [34] Angel L Pey, François Stricher, Luis Serrano, and Aurora Martinez. Predicted effects of missense mutations on native-state stability account for phenotypic outcome in phenylketonuria, a paradigm of misfolding diseases. *The American Journal of Human Genetics*, 81(5):1006–1024, 2007.
- [35] Peter A Kollman, Irina Massova, Carolina Reyes, Bernd Kuhn, Shuanghong Huo, Lillian Chong, Matthew Lee, Taisung Lee, Yong Duan, Wei Wang, et al. Calculating structures and free energies of complex molecules: combining molecular mechanics and continuum models. *Accounts of chemical research*, 33(12):889–897, 2000.
- [36] Jed W Pitera and Peter A Kollman. Exhaustive mutagenesis in silico: multicoordinate free energy calculations on proteins and peptides. *Proteins: Structure, Function, and Bioinformatics*, 41(3):385–397, 2000.

- [37] Paul D Thomas and Ken A Dill. Statistical potentials extracted from protein structures: how accurate are they? *Journal of molecular biology*, 257(2):457–469, 1996.
- [38] Charles W Carter Jr, Brendan C LeFebvre, Stephen A Cammer, Alexander Tropsha, and Marshall Hall Edgell. Four-body potentials reveal protein-specific correlations to stability changes caused by hydrophobic core mutations. *Journal of molecular biology*, 311(4):625–638, 2001.
- [39] Christopher M Topham, N Srinivasan, and Tom L Blundell. Prediction of the stability of protein mutants based on structural environment-dependent amino acid substitution and propensity tables. *Protein engineering*, 10(1):7–21, 1997.
- [40] Dimitri Gilis and Marianne Rooman. Prediction of stability changes upon single-site mutations using database-derived potentials. *Theoretical Chemistry Accounts*, 101:46–50, 1999.
- [41] AJ Bordner and RA Abagyan. Large-scale prediction of protein geometry and stability changes for arbitrary single point mutations. *Proteins: Structure, Function, and Bioinformatics*, 57(2):400–413, 2004.
- [42] Raphael Guerois, Jens Erik Nielsen, and Luis Serrano. Predicting changes in the stability of proteins and protein complexes: a study of more than 1000 mutations. *Journal of molecular biology*, 320(2):369–387, 2002.
- [43] Emidio Capriotti, Piero Fariselli, and Rita Casadio. A neural-network-based method for predicting protein stability changes upon single point mutations. *Bioinformatics*, 20(suppl_1):i63–i68, 2004.
- [44] Hanqun Cao, Cheng Tan, Zhangyang Gao, Guangyong Chen, Pheng-Ann Heng, and Stan Z Li. A survey on generative diffusion model. *arXiv preprint arXiv:2209.02646*, 2022.
- [45] Jianlin Cheng, Arlo Randall, and Pierre Baldi. Prediction of protein stability changes for single-site mutations using support vector machines. *Proteins: Structure, Function, and Bioinformatics*, 62(4):1125–1132, 2006.
- [46] Liang-Tsung Huang, M Michael Gromiha, and Shinn-Ying Ho. Sequence analysis and rule development of predicting protein stability change upon mutation using decision tree model. *Journal of Molecular modeling*, 13:879–890, 2007.
- [47] Piero Fariselli, Pier Luigi Martelli, Castrense Savojardo, and Rita Casadio. Inps: predicting the impact of non-synonymous variations on protein stability from sequence. *Bioinformatics*, 31(17):2816–2821, 2015.
- [48] Lukas Folkman, Bela Stantic, Abdul Sattar, and Yaoqi Zhou. Ease-mm: sequence-based prediction of mutation-induced stability changes with feature-based multiple models. *Journal of molecular biology*, 428(6):1394–1405, 2016.
- [49] Dmitriy Umerenkov, Tatiana I Shashkova, Pavel V Strashnov, Fedor Nikolaev, Maria Sindeeva, Nikita V Ivanisenko, and Olga L Kardymon. Prostata: Protein stability assessment using transformers. *bioRxiv*, pages 2022–12, 2022.
- [50] Ludovica Montanucci, Emidio Capriotti, Yotam Frank, Nir Ben-Tal, and Piero Fariselli. Ddgun: an untrained method for the prediction of protein stability changes upon single and multiple point variations. *BMC bioinformatics*, 20:1–10, 2019.
- [51] Corrado Pancotti, Silvia Benevenuta, Valeria Repetto, Giovanni Birolo, Emidio Capriotti, Tiziana Sanavia, and Piero Fariselli. A deep-learning sequence-based method to predict protein stability changes upon genetic variations. *Genes*, 12(6):911, 2021.
- [52] Gen Li, Shailesh Kumar Panday, and Emil Alexov. Saafec-seq: a sequence-based method for predicting the effect of single point mutations on protein thermodynamic stability. *International journal of molecular sciences*, 22(2):606, 2021.
- [53] Chi-Wei Chen, Meng-Han Lin, Chi-Chou Liao, Hsung-Pin Chang, and Yen-Wei Chu. istable 2.0: predicting protein thermal stability changes by integrating various characteristic modules. *Computational and structural biotechnology journal*, 18:622–630, 2020.
- [54] Douglas EV Pires, David B Ascher, and Tom L Blundell. Duet: a server for predicting effects of mutations on protein stability using an integrated computational approach. *Nucleic acids research*, 42(W1):W314–W319, 2014.

- [55] Yuting Chen, Haoyu Lu, Ning Zhang, Zefeng Zhu, Shuqin Wang, and Minghui Li. Premps: Predicting the impact of missense mutations on protein stability. *PLoS computational biology*, 16(12):e1008543, 2020.
- [56] Bian Li, Yucheng T Yang, John A Capra, and Mark B Gerstein. Predicting changes in protein thermodynamic stability upon point mutation with deep 3d convolutional neural networks. *PLoS computational biology*, 16(11):e1008291, 2020.
- [57] Carlos HM Rodrigues, Douglas EV Pires, and David B Ascher. Dynamut: predicting the impact of mutations on protein conformation, flexibility and stability. *Nucleic acids research*, 46(W1):W350–W355, 2018.
- [58] Castrense Savojardo, Piero Fariselli, Pier Luigi Martelli, and Rita Casadio. Inps-md: a web server to predict stability of protein variants from sequence and structure. *Bioinformatics*, 32(16):2542–2544, 2016.
- [59] Oliver Buß, Jens Rudat, and Katrin Ochsenreither. Foldx as protein engineering tool: better than random based approaches? *Computational and structural biotechnology journal*, 16:25–33, 2018.
- [60] Yves Dehouck, Jean Marc Kwasigroch, Dimitri Gilis, and Marianne Rooman. Popmusic 2.1: a web server for the estimation of protein stability changes upon mutation and sequence optimality. *BMC bioinformatics*, 12(1):1–12, 2011.
- [61] Josef Laimer, Heidi Hofer, Marko Fritz, Stefan Wegenkittl, and Peter Lackner. Maestro-multi agent stability prediction upon point mutations. *BMC bioinformatics*, 16(1):1–13, 2015.
- [62] Daniel J Diaz, Chengyue Gong, Jeffrey Ouyang-Zhang, James M Loy, Jordan Wells, David Yang, Andrew D Ellington, Alex Dimakis, and Adam R Klivans. Stability oracle: A structure-based graph-transformer for identifying stabilizing mutations. *bioRxiv*, pages 2023–05, 2023.
- [63] Kyle A Barlow, Shane 'O Conch' uir, Samuel Thompson, Pooja Suresh, James E Lucas, Markus Heinonen, and Tanja Kortemme. Flex ddg: Rosetta ensemble-based estimation of changes in protein–protein binding affinity upon mutation. *The Journal of Physical Chemistry B*, 122(21):5389–5399, 2018.
- [64] Shuyu Wang, Hongzhou Tang, Peng Shan, Zhaoxia Wu, and Lei Zuo. Pros-gnn: Predicting effects of mutations on protein stability using graph neural networks. *Computational Biology and Chemistry*, 107:107952, 2023.
- [65] Yashas BL Samaga, Shampa Raghunathan, and U Deva Priyakumar. Scones: self-consistent neural network for protein stability prediction upon mutation. *The Journal of Physical Chemistry B*, 125(38):10657–10671, 2021.
- [66] Marcel G Schaap, Feike J Leij, and Martinus Th Van Genuchten. Rosetta: A computer program for estimating soil hydraulic parameters with hierarchical pedotransfer functions. *Journal of hydrology*, 251(3-4):163–176, 2001.
- [67] John Jumper, Richard Evans, Alexander Pritzel, Tim Green, Michael Figurnov, Olaf Ronneberger, Kathryn Tunyasuvunakool, Russ Bates, Augustin Žídek, Anna Potapenko, et al. Highly accurate protein structure prediction with alphafold. *Nature*, 596(7873):583–589, 2021.
- [68] Corrado Pancotti, Silvia Benevenuta, Giovanni Birolo, Virginia Alberini, Valeria Repetto, Tiziana Sanavia, Emidio Capriotti, and Piero Fariselli. Predicting protein stability changes upon single-point mutation: a thorough comparison of the available tools on a new dataset. *Briefings in Bioinformatics*, 23(2):bbab555, 2022.
- [69] Fabrizio Pucci, Katrien V Bernaerts, Jean Marc Kwasigroch, and Marianne Rooman. Quantification of biases in predictions of protein stability changes upon mutations. *Bioinformatics*, 34(21):3659–3665, 2018.
- [70] Yang Zhang and Jeffrey Skolnick. Tm-align: a protein structure alignment algorithm based on the tm-score. *Nucleic acids research*, 33(7):2302–2309, 2005.
- [71] Hehe Fan, Zhangyang Wang, Yi Yang, and Mohan Kankanhalli. Continuous-discrete convolution for geometry-sequence modeling in proteins. In *The Eleventh International Conference on Learning Representations*, 2022.
- [72] Jorge A Vila. Proteins' evolution upon point mutations. *ACS omega*, 7(16):14371–14376, 2022.
- [73] Matthias Fey and Jan Eric Lenssen. Fast graph representation learning with pytorch geometric. *arXiv preprint arXiv:1903.02428*, 2019.

A Dataset details

A.1 Training dataset

We collected samples from PROSTATA [49], subsequently executing TM-Score calculations between each sample pair in the original dataset and those within the S669 and Ssym datasets, intended for evaluative comparisons. Subsequently, samples from the original dataset exhibiting a TM-Score exceeding 0.5 with any sample in the testing datasets were deliberately omitted since such a score indicates a notable structural similarity. This task was performed separately for each testing dataset, ensuring more equitable comparisons without compromising the richness of useful samples. We've depicted the structural similarity distribution between the original dataset and the test datasets in Figure 2, and the distribution after the omission of similar samples is illustrated in Figure 3. The original dataset contains 10544 samples, after filtering similar structures, the subset for testing the S669 dataset has 6951 sample while the subset for the Ssym dataset has 6080. From this, it is evident that the original dataset revealed a substantial number of similar samples, which have been excluded from the filtered datasets. Also, it demonstrates that there are significantly more similar samples between the Ssym dataset and the original training datasets.

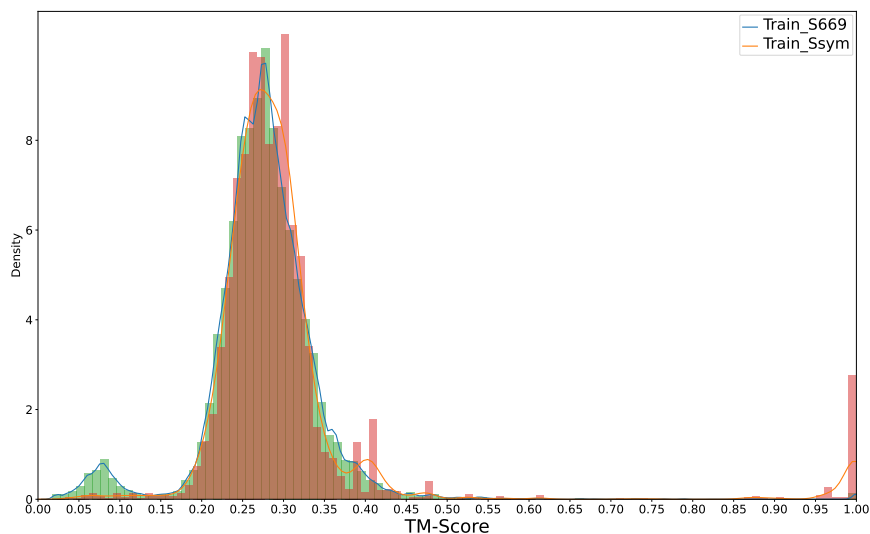


Figure 2: Density distribution of the original dataset towards testing datasets

A.2 Data Cleaning

We first aligned the original sequences and mutated sequences separately with the sequences extracted from PDB file using the Needleman-Wunsch algorithm. However, inconsistency often appears. In order to make strict alignment, we designed a cleaning procedure that deals with the following situations in the aligned sequences. The situations are simplified and visualized in Figure 4.

- The provided sequence has missing residues. As situation 1 in Figure 4 denotes, we amend the position with the corresponding residue in the PDB extracted sequence.
- The PDB extracted sequence has missing residues. As situation 2 in Figure 4 denotes, we following the PDB extracted sequence has the standard and thus omitted the residue from the sequence provided.
- The mutation normally appears as situation 3 denotes in Figure 4. Under these circumstances, we reserve the mutated residue from the provided sequence.

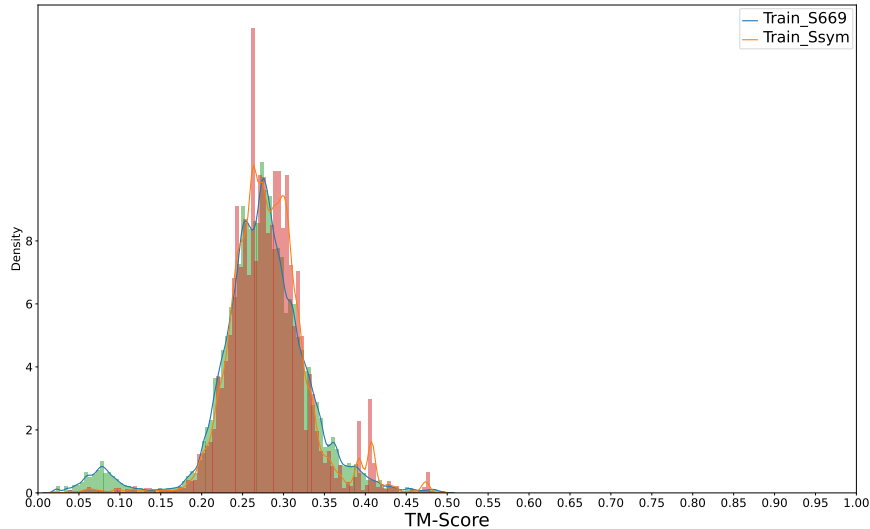


Figure 3: Density distribution of our proposed datasets towards testing datasets

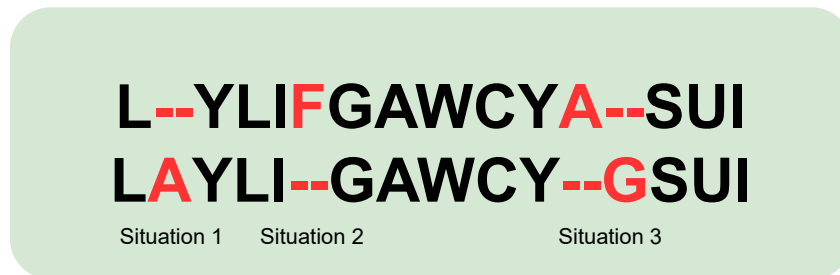


Figure 4: The situations considered in the data cleaning process

It is worth noting that when the neighborhood residue of the mutated position is missing in PDB extracted structures, we are unable to tell if the mutant type is single-point or multiple-point. Therefore, we omitted the sequences under certain circumstances.

A.3 Sample Value Distribution

From our curated dataset, we calculated the distribution of $\Delta\Delta G$ values, the results are visualized in Figure 5. It could be concluded that most values are centered around $[-5, 5]$, with scarce exceptions.

B Implementation Details

In the experiments, we trained the model for 25 epochs with a batch size of 64 and using the OneCycle optimizer with a learning rate of 0.001. The hyperparameters are obtained by conducting 5-fold cross-validation for best-averaged model performance in the validation datasets. The model was implemented based on the standard PyTorch Geometric [73] library and Pytorch Lightning Framework. We ran the models on Intel(R) Xeon(R) Gold 6240R CPU @ 2.40GHz CPU and NVIDIA A100 GPU.

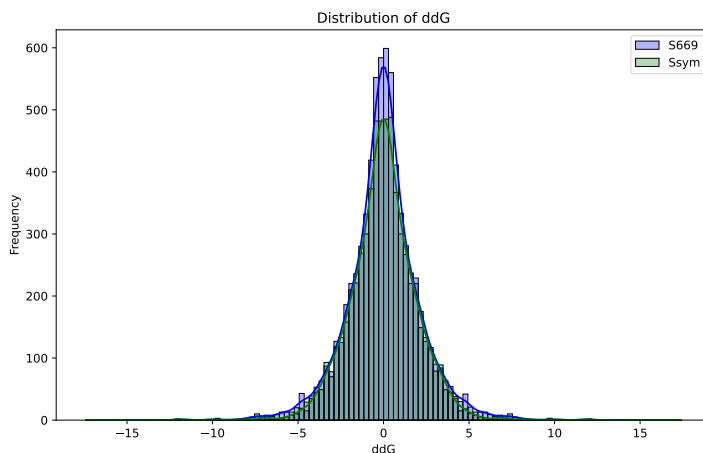


Figure 5: Distribution of DDG in our proposed datasets

C Performance Evaluation on S669 and Ssym Datasets

Beyond the comparison and analysis in Section 3.1, we compared our model with other approaches aiming to predict the thermostability changes upon protein single-point mutation. Since the structures of some methods are complicated to re-implement into our framework to enable fair comparison, and some methods are only offered in the web server, we only tested the model performance on the S669 and Ssym datasets, without applying our training data to them or compare the computational efficiency. The results are shown in Table 4 and Table 5. Some metrics are taken from a comprehensive survey on predicting protein mutation effects [68]. Methods in *Italic* indicate structure-based methods, others are sequence-based ones.

Table 4: The additional evaluation results on the S669 and S669_r datasets.

Method	S669			S669_r		
	PCC \uparrow	RMSE \downarrow	MAE \downarrow	PCC \uparrow	RMSE \downarrow	MAE \downarrow
DDGun	0.41	1.72	1.25	0.38	1.75	1.24
INPS-Seq	0.43	1.51	1.09	0.43	1.53	1.10
<i>DDGun3D</i>	0.43	1.6	1.11	0.41	1.62	1.14
<i>PremPS</i>	0.41	1.5	1.08	0.42	1.49	1.05
<i>MAESTRO</i>	0.5	1.44	1.06	0.2	2.1	1.66
<i>PoPMuSiC</i>	0.41	1.51	1.09	0.24	2.09	1.64
<i>ThermoNet</i>	0.39	1.62	1.17	0.38	1.66	1.23
Ours	0.51	1.46	1.07	0.51	1.46	1.07

Table 5: The additional evaluation results on the Ssym and Ssym_r datasets.

Method	Ssym			Ssym_r		
	PCC \uparrow	RMSE \downarrow	MAE \downarrow	PCC \uparrow	RMSE \downarrow	MAE \downarrow
DDGun	0.51	1.51	1.12	0.51	1.51	1.12
INPS-Seq	0.5	1.53	1.11	0.51	1.52	1.11
<i>DDGun3D</i>	0.58	1.45	1.04	0.56	1.49	1.07
<i>PremPS</i>	0.81	1.05	0.7	0.73	1.21	0.83
<i>MAESTRO</i>	0.6	1.37	0.95	0.25	2.27	1.73
<i>PoPMuSiC</i>	0.65	1.27	0.9	0.28	2.25	1.71
<i>ThermoNet</i>	0.45	1.66	1.16	0.39	1.73	1.21
Ours	0.47	1.45	1.05	0.47	1.45	1.05

It could be concluded from the results that our model demonstrates consistent performance across both datasets and their reversed counterparts. It is competitive in all metrics but is occasionally surpassed by models such as *PremPS* [55] and *MAESTRO* [61] in certain metrics. The strength of our model lies in its generalizability since there is no information leakage between the training dataset and the testing dataset while others exist or are unknown. Also, our model stands out for its consistent performance, while some other models exhibit more variability between datasets. Furthermore, numerous methods display comparable performance on these datasets. This underscores the importance of broadening the data spectrum and constructing more robust datasets for future research.